· Article · Advances in Polar Science
doi: 10.13679/j.advps.2019.0019 March 2020 Vol. 31 No. 1: 14-25

Evaluation of ArcIOPS sea ice forecasting products during the ninth CHINARE-Arctic in summer 2018

LIANG Xi[1*], ZHAO Fu[1], LI Chunhua[1], ZHANG Lin[1] & LI Bingrui[2]

[1] Key Laboratory of Research on Marine Hazards Forecasting, National Marine Environmental Forecasting Center, Beijing 100081, China;
[2] Polar Research Institute of China, Shanghai 200136, China

Received 13 May 2019; accepted 27 August 2019; published online 6 March 2020

Abstract Numerical sea ice forecasting products during the ninth Chinese National Arctic Research Expedition (9th CHINARE-Arctic) from Arctic Ice Ocean Prediction System (ArcIOPS) of National Marine Environmental Forecasting Center of China are evaluated against satellite-retrieved sea ice concentration data, *in-situ* sea ice thickness observations, and sea ice products from Pan-Arctic Ice Ocean Modeling and Assimilation System (PIOMAS). The results show that ArcIOPS forecasts reliable sea ice concentration and thickness evolution. Deviations of the 168 h sea ice concentration and thickness forecasts with respect to the observations are less than 0.2 and 0.36 m. Comparison between outputs of the latest version of ArcIOPS and that of its previous version shows that the latest version has a substantial improvement on sea ice concentration forecasts due to data assimilation of new observational component, the sea surface temperature. Meanwhile, the sea ice volume product of the latest version is more close to the PIOMAS product. In the future, with more and more kinds of observations to be assimilated, the high-resolution version of ArcIOPS will be put into operational running and benefit Chinese scientific and commercial activities in the Arctic Ocean.

Keywords **ArcIOPS, CHINARE-Arctic, sea ice forecasts, validation**

Citation: Liang X, Zhao F, Li C H, et al. Evaluation of ArcIOPS sea ice forecasting products during the ninth CHINARE-Arctic in summer 2018. Adv Polar Sci, 2020, 31(1): 14-25, doi: 10.13679/j.advps.2019.0019

1 Introduction

Sea ice motion in the marginal sea ice zone is closely affected by surface wind (Thorndike and Colony, 1982). Cyclone activities strongly perturb sea ice distribution by direct momentum forcing and heat exchanging (Yang et al., 2004). The ninth Chinese National Arctic Research Expedition (9th CHINARE-Arctic) started on 20 July 2018 with a duration of 69 d, multidisciplinary investigations were carried out in Marginal sea Ice zone of the Pacific Sector of the Arctic Ocean (MIPSAO). The icebreaker R/V *Xuelong* navigated in the ice-covered area of the MIPSAO during all of August. Driven by frequent cyclonic processes, sea ice conditions in the MIPSAO have rapid daily variations (Crane, 1983). Numerical sea ice forecasting information, from the Arctic Ice Ocean Prediction System (ArcIOPS) of the National Marine Environmental Forecasting Center (NMEFC) of China, was provided to the icebreaker for reference purpose in planning its route and avoiding the potential risk of thick ice.

ArcIOPS (Mu et al., 2019), established in 2017, is an operational ensemble forecasting system to predict short-term evolution of the Arctic sea ice and ocean states. The numerical sea ice-ocean model of ArcIOPS is an Arctic configuration of the Massachusetts Institute of Technology general circulation model (MITgcm, Marshall et al., 1997). The data assimilation model of ArcIOPS is based on a member from the family of the Ensemble Kalman Filter

* Corresponding author, E-mail: liangx@nmefc.cn

(EnKF, Evensen, 1994) schemes. The first version of ArcIOPS (ArcIOPS v1.0) assimilates available satellite-retrieved sea ice concentration and thickness data. Sea ice thickness forecasting products from ArcIOPS v1.0 were provided to the eighth Chinese National Arctic Research Expedition (8th CHINARE-Arctic), and are believed to have played an important role in the successful passage of R/V *Xuelong* through the Central Arctic for the first time during the summer of 2017. In 2018, ArcIOPS v1.0 was upgraded to the latest version (ArcIOPS v1.1). Satellite-retrieved sea ice concentration, sea ice thickness, as well as sea surface temperature (SST) data in ice free areas, are assimilated into ArcIOPS v1.1. From 1 January 2018 on, ArcIOPS v1.1 has been run operationally for more than one year in the NMEFC. Outputs from ArcIOPS v1.1 include ensemble-mean 168 h forecasts of sea ice concentration, sea ice thickness, sea ice drift, ocean temperature and salinity. Sea ice concentration, thickness, and drift forecasting products were offered to the 9th CHINARE-Arctic.

In this paper, we evaluate the numerical sea ice forecasting products from ArcIOPS v1.1 during the 9th CHINARE-Arctic using *in-situ* sea ice thickness observations, satellite sea ice concentration data from independent sensors, and model results from Pan-Arctic Ice Ocean Modeling and Assimilation System (PIOMAS, Zhang and Rothrock, 2003). Comparison between outputs of ArcIOPS v1.1 and that of ArcIOPS v1.0 is also presented. During the 9th CHINARE-Arctic, R/V *Xuelong* passed through the Bering Strait into the Arctic Ocean on 30 July, thus our study focuses on August and September in 2018. The rest of the paper is organized as follows: a brief description of ArcIOPS v1.1, its upgrades related to ArcIOPS v1.0, and data used for validation are given in section 2. The main results are presented in section 3. Discussion and conclusion are given in section 4.

2 Methods

2.1 Arctic Ice-Ocean Prediction System v1.1

The numerical sea ice-ocean model of ArcIOPS is an Arctic configuration of the MITgcm, with its open boundaries close to 55°N in both the Atlantic and Pacific sectors (Nguyen et al., 2011; Liang and Losch, 2018). The ocean model within the Arctic configuration uses Arakawa C grid and Z coordinates. The model grid is locally orthogonal. The ocean model includes 420×384 horizontal grid points with an averaged horizontal resolution of 18 km, and 50 vertical layers with vertical resolution increasing from 10 m near the surface to 456 m near the bottom. The sea ice model within the Arctic configuration uses viscous-plastic dynamics and zero-layer thermodynamics (Semtner, 1976), and shares the same horizontal grid with the ocean model. The sea ice model includes two sea ice thickness categories: open water and sea ice (Losch et al., 2010).

The data assimilation model of ArcIOPS uses an ensemble-based Localized Error Subspace Transform Kalman Filter (LESTKF, Nerger et al., 2012), which is implemented in the Parallel Data Assimilation Framework (PDAF, Nerger and Hiller, 2013). With dynamical state error covariances, the EnKF data assimilation schemes are suitable for sea ice data assimilation (Lisæter et al., 2003; Sakov et al., 2012; Yang et al., 2014, 2015; Liang et al., 2017; Mu et al., 2018a). The LESTKF is one member from the family of EnKFs, and has some advanced features, such as high accuracy, low computational consumption and outstanding efficiency.

ArcIOPS v1.1 employs almost the same offline data assimilation strategy as ArcIOPS v1.0, but with three main upgrades. Firstly, in addition to the assimilations of sea ice concentration and sea ice thickness, the satellite-retrieved Group for High-Resolution SST Multi-Product Ensemble (GMPE) SST data in ice free areas was assimilated in ArcIOPS v1.1 (Liang et al., 2019). Secondly, to moderately amplify influences of the observations, the localized radius has been increased from 126 km of ArcIOPS v1.0 to 216 km of ArcIOPS v1.1. Thirdly, the CS2SMOS sea ice thickness data (Ricker et al., 2017) used in ArcIOPS v1.0 is replaced by the Soil Moisture Ocean Salinity (SMOS) sea ice thickness data (Tian-Kunze et al., 2014) and the European Space Agency (ESA) satellite mission CryoSat-2 sea ice thickness data (Wingham et al., 2006; Laxon et al., 2013; Ricker et al., 2014) and applied in ArcIOPS v1.1. The CS2SMOS sea ice thickness data is a derived product which combines the SMOS and CryoSat-2 sea ice thickness data using an optimal interpolation scheme. The CS2SMOS data covers both thin ice and thick ice in the Arctic.

The transition from ArcIOPS v1.0 to ArcIOPS v1.1 was implemented on 1 January 2018. The operational diagram of ArcIOPS v1.1 in 2018 is shown in Figure 1. The ensemble includes 12 parallel runs, R01 to R12. The initial model states on 1 January are directly taken from ArcIOPS v1.0. From 1 January to 30 April and from 1 October to 31 December, the SMOS sea ice thickness data, the CryoSat-2 sea ice thickness data, the Advanced Microwave Scanning Radiometer 2 (AMSR2) sea ice concentration data (Spreen et al., 2008), and the GMPE SST data are assimilated into ArcIOPS v1.1. The SMOS and Cryosat-2 sea ice thickness observations are unavailable in the melt season, thus from 1 May to 30 September only the AMSR2 sea ice concentration and GMPE SST data are assimilated into ArcIOPS v1.1. Due to the long-term sea ice memory of melting-freezing processes (Day et al., 2014; Mu et al., 2018b), the sea ice thickness assimilation in the first four months of 2018 provides a substantial guarantee for the sea ice thickness forecasts in the following several months.

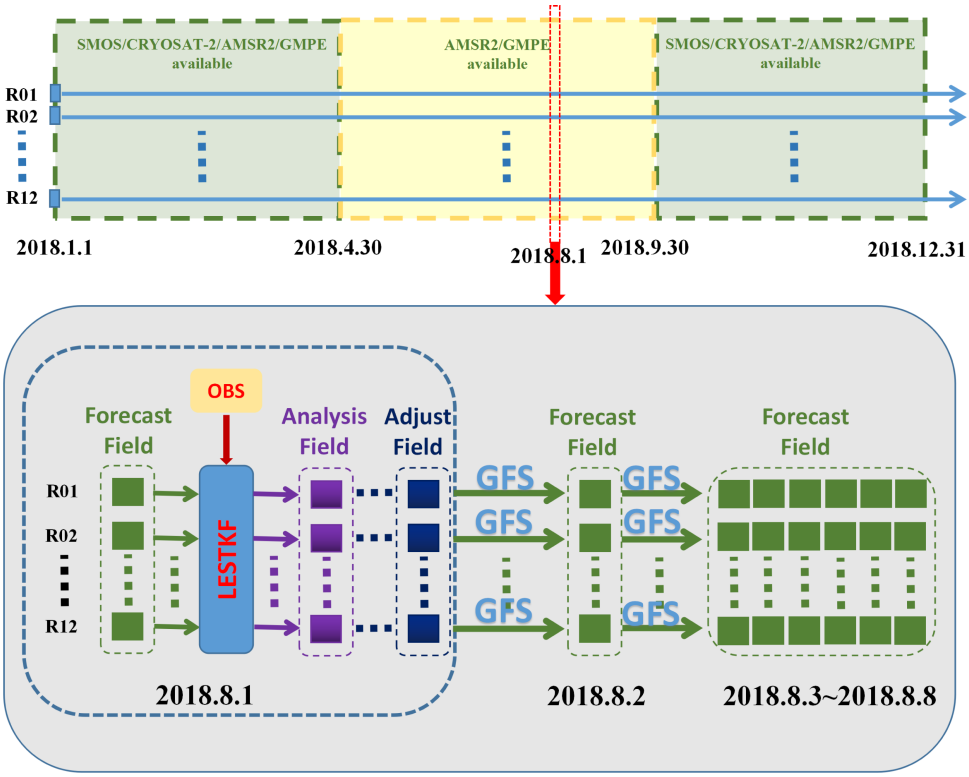

Figure 1 The ArcIOPS v1.1 operational diagram in 2018. The top panel shows the time window with different observational data to be assimilated. The red dot-solid arrow denotes the flow chart on 1 August which is specified in the bottom panel. R01 to R12 denote 12 parallel runs. The green, purple, and cyan squares denote sea ice-ocean forecast, analysis, and adjustment states corresponding to the 12 parallel runs. The sea ice-ocean adjustment states on 1 August are driven by the GFS atmospheric forcing for 24 h to get the forecast states on 2 August, which are used in the next data assimilation cycle, and then for another 144 h to get the forecast states from 3 August to 8 August. SMOS = Soil Moisture Ocean Salinity; AMSR2 = Advanced Microwave Scanning Radiometer 2; GMPE = Group for High-Resolution SST Multi-Product Ensemble; OBS = observations; LESTKF = Localized Error Subspace Transform Kalman Filter; GFS = Global Forecast System.

A complete ensemble data assimilation cycle normally includes three phases: analysis, adjustment and forecast. Taking the ensemble data assimilation cycle on 1 August as an example, in the analysis phase the data assimilation model collects the sea ice-ocean model states of all the runs and available observations. Note here the sea ice-ocean model states include sea ice concentration, sea ice thickness, and upper 200 m ocean temperature. Then a loop over all model grid points is performed for the local analysis. The LESTKF algorithm transforms the ensemble of the model states into the analysis states by incorporating the observations into the model states. For each model grid point to be updated, only observations within the localized radius around the updating grid point are used and a localization weighting algorithm is applied to the observations. Meanwhile, a forgetting factor of 0.9 is used in the LESTKF algorithm to increase the ensemble spread. In the adjustment phase, physical constraints and relationships among model variables are applied to the analysis states, for example, sea ice thickness is set to 0 whenever the sea ice concentration is 0, sea ice concentration and thickness are set to 0 whenever the surface ocean temperature is warmer than the surface freezing point, and then the adjustment states are obtained. In the forecast phase, all the runs with the adjustment states as initial fields are integrated for 168 h separately using the GFS atmospheric forcing data. Ensemble-mean daily sea ice and ocean forecasts from 2 August to 8 August are outputted. The forecasting states on 2 August are used as the model states in the following data assimilation cycle.

2.2 Data sets

Daily AMSR2 sea ice concentration data, daily SMOS sea ice thickness data in thin ice area (< 1 m) and monthly Cryosat-2 sea ice thickness data are used for the assimilation. The AMSR2 sea ice concentration data (available at http://data.meereisportal.de/data/iup/hdf/), provided by the University of Bremen, are derived from Global Change Observation Mission – Water satellite brightness temperature data with a horizontal resolution of 6.25 km using the ARTIST Sea Ice (ASI) algorithm. Sponsored by the ESA, the SMOS sea ice thickness data are also retrieved from satellite brightness temperature data (available at http://data.meereisportal.de/data/iup/smos/). A

sea ice thermodynamic model and a three-layer radiative transfer model are used to convert the SMOS brightness temperature to sea ice thickness (Kaleschke et al., 2010, 2012). The SMOS data quality is guaranteed in thin ice areas. The Cryosat-2 sea ice thickness data are retrieved from radar altimetry measurements of sea ice freeboard (available at http://data.meereisportal.de/data/cryosat2/). Freeboard measurements can be converted to sea ice thickness under hydrostatic equilibrium assumption (Kwok et al., 2009; Laxon et al., 2013). Sea ice thickness uncertainties are also included in the Cryosat-2 data set. In ArcIOPS v1.1, the Cryosat-2 sea ice thickness and its uncertainties are assimilated on the daily basis with the daily values coming from linear interpolation of the monthly values.

Daily GMPE SST data and its uncertainties for the assimilation are provided by the United Kingdom Met Office (UKMO). The GMPE SST data is a near-real-time Level 4 satellite-retrieved product which covers ice free areas with a horizontal resolution of 1/4 degree (available at http://marine.copernicus.eu/, product identifier: SST_GLO_SST_L4_NRT_OBSERVATIONS_010_005). The sea ice concentration, thickness, SST observations, as well as available uncertainties, are interpolated onto the MITgcm model grid. The uncertainties of the AMSR2 and SMOS data are unified 25% and 0.25 m for the whole model domain based on our pre-operational tuning.

To evaluate sea ice concentration forecasts, sea ice concentration data from the EUMETSAT Ocean and Sea Ice Satellite Application Facility (OSISAF, Eastwood et al., 2011) are used (available at http://osisaf.met.no/p/ice/, product: OSI-401-b). The OSISAF data have a horizontal resolution of 10 km and are independent of the AMSR2 sea ice concentration data, because the OSISAF and AMSR2 data are measured by different sensors. The OSISAF data are retrieved by a hybrid algorithm that combines the Bootstrap algorithm in frequency mode (Comiso et al., 1997) and the Bristol algorithm (Smith, 1997), which is different from the ASI algorithm used by the AMSR2 data.

To evaluate sea ice thickness forecasts, *in-situ* sea ice thickness observations along the navigation trajectory of R/V *Xuelong* are used. The *in-situ* observations are available for all of August. The sea ice thickness observations are automatically recorded by the ship-borne Geonics EM31 Ground Conductivity Meter (EM31). The EM31 maps the sea ice thickness using a patented electromagnetic inductive technique that makes the measurements without direct contact. The instrument measures the quadrature of the secondary magnetic field, which can be converted to an apparent conductivity and hence sea ice thickness. The ship-borne EM31 samples sea ice thickness along the navigation trajectory of R/V *Xuelong* at a sampling interval of 1 s. The EM31 sea ice thickness observations are calibrated following Guo et al. (2008). Note that artificial uncertainties exist when comparing the EM31 observations with model values, because our modeled ice thickness is a mean value of each model grid with an area of 18 km^2 while the icebreaker prefers to navigate in thinner ice regions. The EM31 observations are smoothed into a daily mean value for the comparison.

Additionally, sea ice products from the Pan-Arctic Ice Ocean Modeling and Assimilation System (PIOMAS, Zhang and Rothrock, 2003) are used for the comparison. The PIOMAS, developed at Applied Physics Laboratory of the University of Washington, assimilates the near-real-time sea ice concentration data from the National Snow and Ice Data Center (NSIDC) and SST data from the NCEP/NCAR Reanalysis by nudging and optimal interpolation. Atmospheric forcing to drive the PIOMAS, include surface wind, surface air temperature, cloud cover to compute solar and long wave radiation. These are also specified from the NCEP/NCAR Reanalysis. Total sea ice volume in the Arctic Ocean, spatial mean sea ice thickness over areas where ice is thicker than 0.15 m, and monthly mean sea ice thickness on the PIOMAS model grid are produced up to date and used in our study (available at http://psc.apl.uw.edu/research/projects/arctic-sea-ice-volume-anomaly/data/).

3 Results

To give a first impression, we show the monthly mean analyzed sea ice state deviation between the ArcIOPS v1.1 and ArcIOPS v1.0 runs during the 9th CHINARE-Arctic. Here analyzed sea ice state is the adjustment state in the data assimilation cycle (Figure 2). The influences of the SST data assimilation on the sea ice concentration and thickness states are significant in the marginal sea ice zone, especially in the MIPSAO. The SST assimilation induces the melting of sea ice in the MIPSAO, which indicates that the correction of ocean surface temperature is toward warming the ocean surface.

3.1 Comparison with the OSISAF data

ArcIOPS v1.1 outputs 168 h sea ice concentration forecasts. To quantitatively evaluate the sea ice concentration forecasting capacity, the time evolution of sea ice concentration root mean square error (RMSE) of the ArcIOPS forecasts with respect to the OSISAF data are shown in Figure 3. It is straightforward that the sea ice concentration forecasting capacities of both the two ArcIOPS versions decrease as the forecasting lead time increases. During the 9th CHINARE-Arctic, the mean sea ice concentration RMSE between the ArcIOPS v1.0 forecasts and the OSISAF data increases from 0.17 for the 24 h lead forecasts to 0.18 for the 72 h lead forecasts, 0.19 for the 120 h lead forecasts, and 0.20 for the 168 h lead forecasts (Table 1). It is remarkable that by involving SST data assimilation, the sea ice concentration forecasting capacity of ArcIOPS v1.1 improves (Figure 3). Compared with the ArcIOPS v1.0 forecasts, the mean sea ice

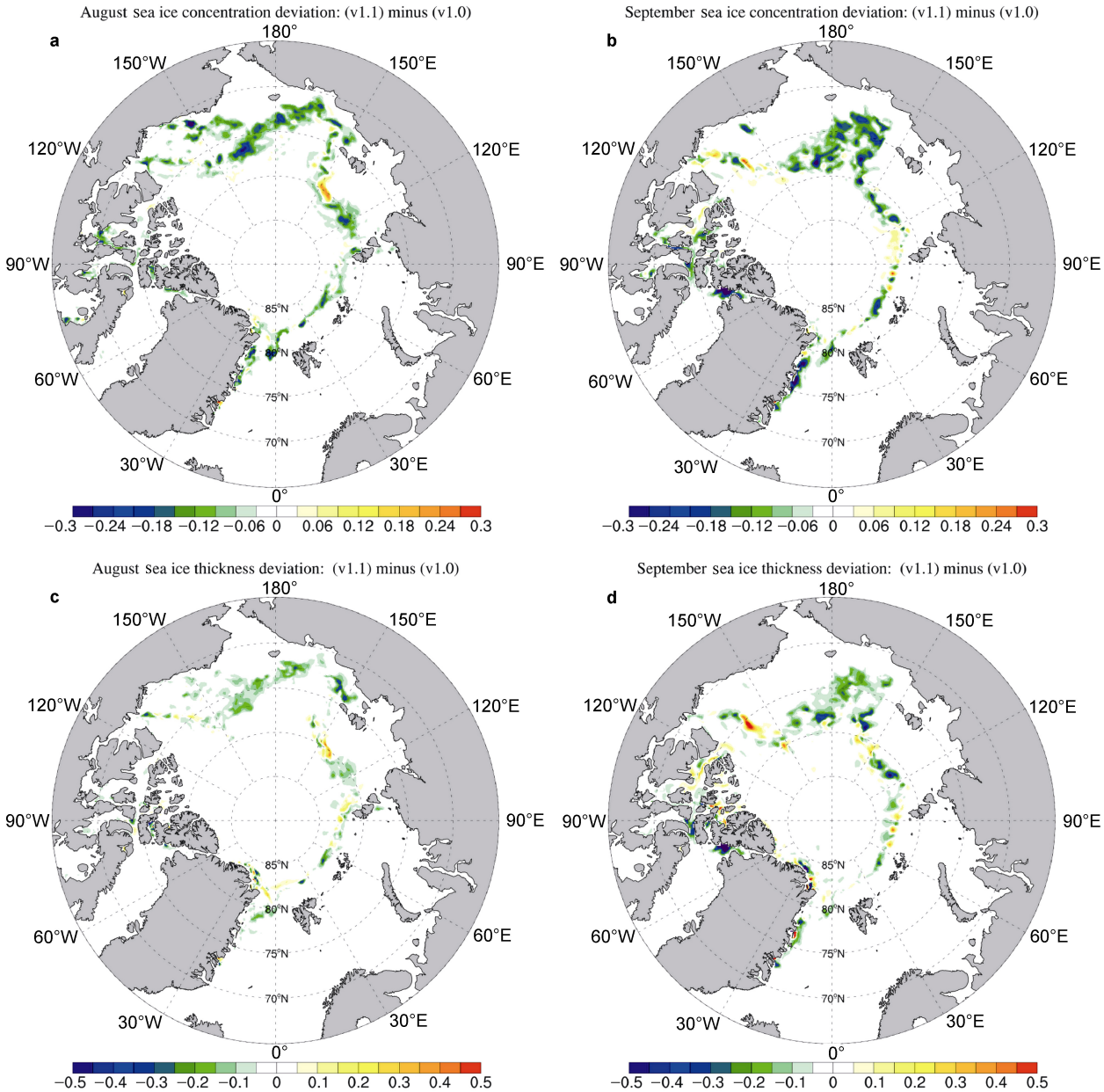

Figure 2 The deviation of analyzed sea ice concentration (**a**, **b**) and thickness (**c**, **d**) between the ArcIOPS v1.1 and v1.0 products. The left and right panels denote August-mean and September-mean.

concentration RMSE between the ArcIOPS v1.1 forecasts and the OSISAF data reduces by more than 0.01 for all the different lead times (Table 1).

Time evolution of the sea ice concentration RMSE shows that both the two ArcIOPS versions forecast relatively larger sea ice concentration errors from 15 August to 5 September than that from 1 August to 10 August. Focused on the ArcIOPS v1.1 forecasts, snapshots of the 24 h lead forecasts and the OSISAF data on 1 August and 1 September are shown in Figure 4. Generally speaking, on 1 August ArcIOPS v1.1 forecasts similar sea ice extent to the observation, but higher sea ice concentration in the marginal sea ice zone than the observation (Figure 4e). While on 1 September, ArcIOPS v1.1 forecasts higher sea ice concentration both in the marginal sea ice zone and in the pack ice zone than the observation (Figure 4f). The growth of the sea ice concentration error during August partly comes from the imperfect parameterization of sea ice melting processes in the numerical sea ice-ocean model. Although with the correction of AMSR2 sea ice concentration data assimilation, the sea ice dynamic and thermodynamic processes in the numerical sea ice-ocean model is still a crucial factor in accurate sea ice prediction.

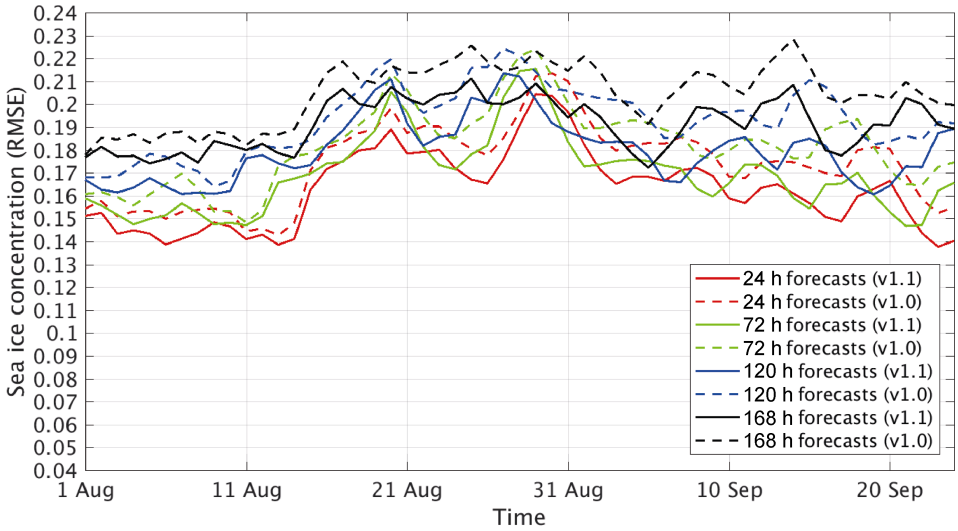

Figure 3 Time evolutions of the RMSE of sea ice concentration with respect to the OSISAF data over the whole model domain. The solid and dashed lines denote the ArcIOPS v1.1 and v1.0 products. The red, green, blue, and black lines denote the 24 h, 72 h, 120 h, and 168 h lead forecasts.

Table 1 Mean RMSE of the sea ice concentration forecasts with respect to the OSISAF data during the 9th CHINARE-Arctic

	Lead time			
	24 h	72 h	120 h	168 h
ArcIOPS v1.1	0.16	0.17	0.18	0.19
ArcIOPS v1.0	0.17	0.18	0.19	0.20

To distinguish the regional difference of the forecasting capacity, spatial distributions of the sea ice concentration RMSE with respect to the OSISAF data of the 24 h forecasts of ArcIOPS and the AMSR2 data are shown during the 9th CHINARE-Arctic in Figure 5. For the forecasts of the two ArcIOPS versions, large sea ice concentration RMSEs exist in the MIPSAO and near to the sea ice edge in the Atlantic sector of the Arctic Ocean (Figures 5a and 5b). Regional difference of the forecasting capacity is closely linked with the sea ice concentration deviation between the assimilated AMSR2 data and the OSISAF data (Figure 5c). Furthermore, compared with the ArcIOPS v1.0 forecasts, the sea ice concentration RMSE between the ArcIOPS v1.1 forecasts and the OSISAF data decreases both in the MIPSAO and near to the sea ice edge in the Atlantic sector of the Arctic Ocean. The spatial patterns of the sea ice concentration RMSE with respect to the OSISAF data of the 72 h, 120 h and 168 h lead forecasts are similar to that of the 24 h lead forecasts (not shown).

3.2 Comparison with the EM31 observations

R/V *Xuelong* navigated in the ice-covered region during all of August, and *in-situ* EM31 sea ice thickness observations along the navigation trajectory provide a direct reference for the evaluation of the sea ice thickness forecasts. Figure 6 shows the navigation trajectory of R/V *Xuelong* during August. The icebreaker meandered in the MIPSAO south of 80°N before 11 August, and arrived at the northernmost workstation near to 85°N on 20 August. The navigation trajectory between the northernmost workstation and 80°N is outside of the predicted 1.5 m thick sea ice zone. The ArcIOPS v1.1 predicted edge of 1.5 m sea ice thickness is an important piece of information for vessels navigated in the Arctic Ocean. During 8th CHINARE-Arctic, the R/V *Xuelong* navigated through the central Arctic Passage along ArcIOPS v1.0 predicted edge of 1.5 m sea ice zone (Bing Zhu, R/V *Xuelong* Captain, personal communication).

Comparison between the sea ice thickness forecasts and observations shows that the two ArcIOPS versions forecast reliable sea ice thickness evolution along the navigation trajectory during August. For the two ArcIOPS versions, both the August mean sea ice thickness RMSEs between the 24 h lead forecasts and observations are below 0.34 m, and a deviation less than 0.03 m is produced between the 24 h and 168 h lead forecasts (Table 2).

Because the SST data assimilation only generates a significant difference in the marginal sea ice zone, the sea ice thickness forecasts of the two ArcIOPS versions do not obviously diverge from 10 August to 28 August when the icebreaker is in the pack ice zone (Figure 7). From 6 August to 8 August and from 29 August to 31 August, the two ArcIOPS versions produce notable differences between the sea ice thickness forecasts which come from the assimilation of ocean surface temperature. For example, ArcIOPS v1.0 predicts that the icebreaker navigates in 0.3–0.5 m thick sea ice on 30 August, while ArcIOPS v1.1 predicts that the icebreaker navigates in an ice-free area on 30 August. The SST assimilation on 29 August leads to the melting of sea ice in the area around the navigation trajectory of 30 August, although the observations on 30 August show that the SST assimilation deteriorates the sea

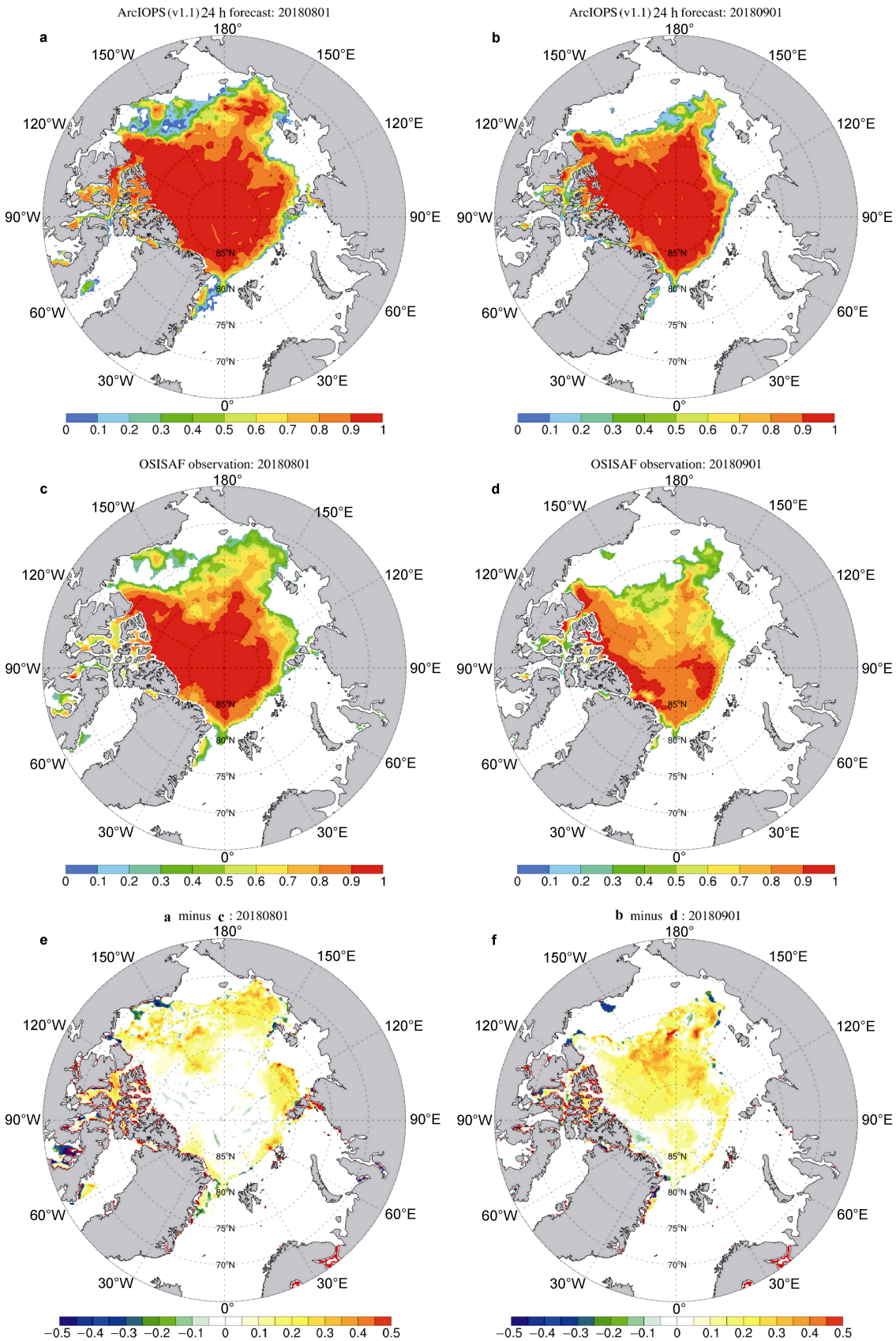

Figure 4 Sea ice concentration on 1 August (**a**, **c**, **e**) and 1 September (**b**, **d**, **f**). The top, middle, and bottom panels denote the 24 h lead forecasts of ArcIOPS v1.1, the OSISAF observations, and the deviation between the top and middle panels, respectively.

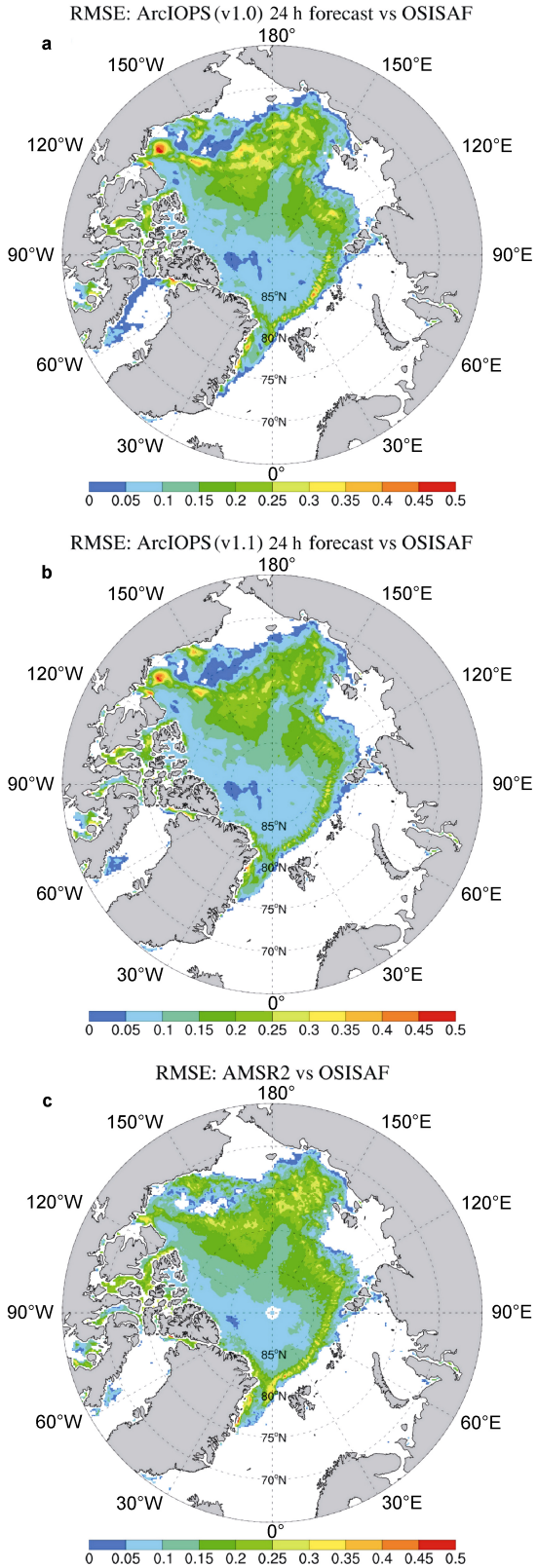

Figure 5 Spatial distributions of the RMSE of sea ice concentration with respect to the OSISAF data of the 24 h lead forecasts of ArcIOPS v1.0 (**a**), the 24 h lead forecasts of ArcIOPS v1.1 (**b**), and the assimilated AMSR2 data (**c**). Values are calculated over the entire duration of the 9th CHINARE-Arctic.

ice thickness forecasts. This negative effect partly comes from the uncertainty of satellite SST data near to sea ice edge.

3.3 Comparison with the PIOMAS product

The PIOMAS is a numerical model with components for sea ice, ocean and data assimilation. Satellite sea ice concentration and reanalyzed SST data are assimilated into the PIOMAS to improve sea ice thickness estimates. The PIOMAS product has been validated through comparisons with observations from US Navy submarines, oceanographic moorings, and satellites. As a reliable product, the PIOMAS sea ice thickness data have been widely used as a reference data set for Arctic sea ice thickness comparisons.

We compare analyzed sea ice products from the two ArcIOPS versions with the PIOMAS product. Sea ice thickness evolution along the navigation trajectory of R/V *Xuelong* shows that the pack ice in the PIOMAS product isthicker than that in the ArcIOPS product by 0.1–0.3 m. It is notable that sea ice thickness forecasts from ArcIOPS v1.1 are more close to those from the PIOMAS product in the marginal sea ice zone (Figure 7). Figure 8 shows time evolution of total sea ice volume and spatial mean sea ice thickness over the Arctic Ocean. The two ArcIOPS versions simulate similar sea ice volume evolution to the PIOMAS product. The sea ice volume evolution from ArcIOPS v1.1 is slightly closer to that from the PIOMAS product. For the sea ice thickness simulation, the two ArcIOPS versions produce thinner sea ice than the PIOMAS product over the Arctic Ocean, the spatial mean deviation is less than 0.2 m. Compared with the ArcIOPS v1.0 simulation, the ArcIOPS v1.1 simulates thicker sea ice by assimilating SST observations and also a sea ice thickness evolution curve more close to that from the PIOMAS product.

Monthly mean sea ice thickness distributions of August and September are shown in Figure 9. Generally speaking, the spatial distributions of sea ice thickness from ArcIOPS v1.1 are similar to that from the PIOMAS product, except that a displacement of the multiyear sea ice extent exists. Large sea ice thickness differences between the ArcIOPS v1.1 and PIOMAS products are located in the multiyear sea ice zone near to the Canadian Arctic Archipelago. It is unsurprising that the sea ice thickness distributions from ArcIOPS v1.1 disagree here because the assimilated Cryosat-2 sea ice thickness data are retrieved from remotely-sensed measurements from a polar orbiting satellite, which means that the monthly Cryosat-2 sea ice thickness is composed of many patches along the satellite tracks.

4 Discussion and conclusion

In this paper, evaluation of the ArcIOPS sea ice forecasts during the 9th CHINARE-Arctic has been carried out

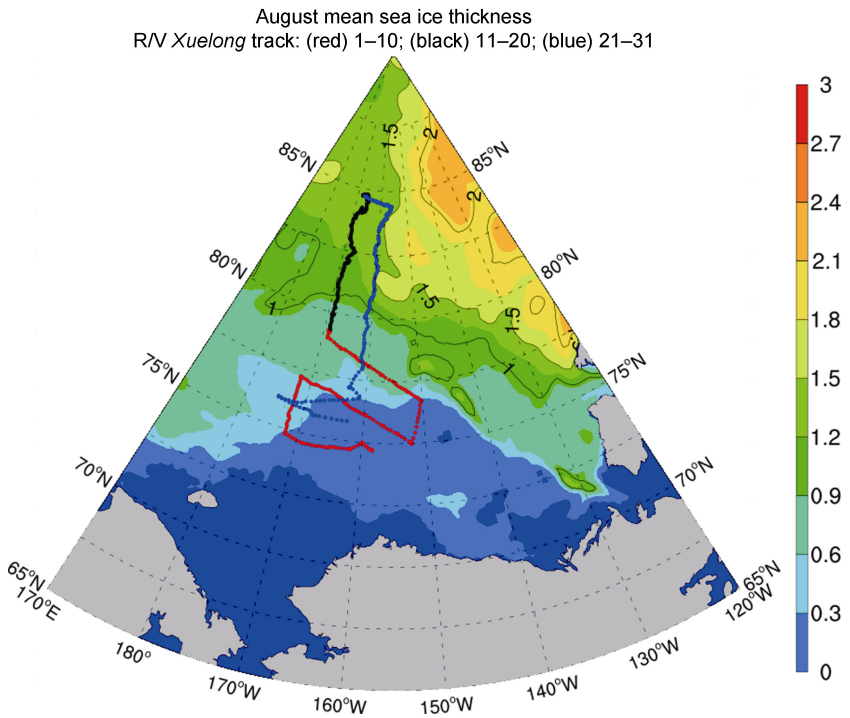

Figure 6 August-mean analyzed sea ice thickness in the Pacific sector of the Arctic Ocean and the navigation trajectory of R/V *Xuelong*. The red, black, and blue dotted lines denote the navigation trajectories of 1–10, 11–20, and 21–31 August, respectively.

Table 2 Mean RMSE of the sea ice thickness forecasts with respect to the EM31 data along the navigation trajectory of R/V *Xuelong* during August 2018

	Lead time			
	24 h	72 h	120 h	168 h
ArcIOPS v1.1	0.33 m	0.34 m	0.35 m	0.36 m
ArcIOPS v1.0	0.33 m	0.34 m	0.34 m	0.35 m

against *in-situ* sea ice thickness observations, satellite-retrieved sea ice concentration data and sea ice products from the PIOMAS. It is found that ArcIOPS v1.1 has a reliable short-term sea ice forecasting capacity. The mean RMSE of 168 h sea ice concentration lead forecasts with respect to the OSISAF data is less than 0.2. The mean RMSE of 168 h sea ice thickness lead forecasts with respect to the EM31 observations along the navigation trajectory of R/V *Xuelong* during August 2018 is less than 0.36 m. The analyzed sea ice volume evolution from ArcIOPS v1.1 is close to that from the PIOMAS while spatial mean sea ice thickness from ArcIOPS v1.1 is thinner than that from the PIOMAS with a mean deviation of 0.1 m.

The difference of the forecasting capacity between ArcIOPS v1.1 and v1.0 has also been presented. Compared with the ArcIOPS v1.0 forecasts, ArcIOPS v1.1 has an improvement on sea ice concentration forecasts, the sea ice thickness forecasts do not show substantial improvement compared with the *in-situ* observations, which may be attributed to the representative limitation of along trajectory sea ice thickness observations, but are closer to the PIOMAS's sea ice thickness product. Actually in another research (Liang et al., 2019), we found that assimilating SST data in addition to sea ice concentration and sea ice thickness not only improves the upper ocean temperature simulation, but also improves the sea ice edge and sea ice extent simulations, as well as the sea ice thickness in the marginal sea ice zone. The simulated sea ice volume from ArcIOPS v1.1 is also closer to the PIOMAS's sea ice volume product.

Upgrades from the ArcIOPS v1.0 to ArcIOPS v1.1 include the SST data assimilation in ice free areas, the replacement of the CS2SMOS sea ice thickness data by the original Cryosat-2 and SMOS data, and enlargement of the localized radius in the data assimilation algorithm. The additional SST data assimilation provides a substantial improvement on the sea ice concentration forecasts in the marginal sea ice zone. Involving ocean data assimilation in a sea ice-ocean prediction system is essential to protect the positive effects of sea ice data assimilation. Satellite-retrieved observations with advantages of board spatial coverage and temporal continuity are optimal data for assimilation in numerical sea ice forecasting systems. However there are still large uncertainties in satellite data, especially the sea ice thickness observations. The accuracy of satellite sea ice thickness data is a choke point of state of the art sea ice forecasting systems. Developing sea ice thickness retrieving algorithm is urgently needed by the sea ice research community.

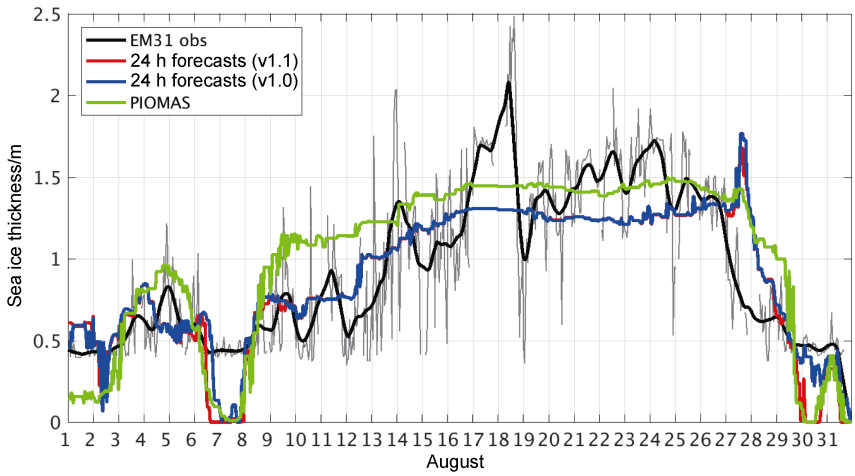

Figure 7 The sea ice thickness evolutions along the navigation trajectory of R/V *Xuelong* in August. The red, blue, green, black, and gray lines denote the ArcIOPS v1.1 forecasts, the v1.0 forecasts, the PIOMAS products, the daily mean and original EM31 observations, respectively.

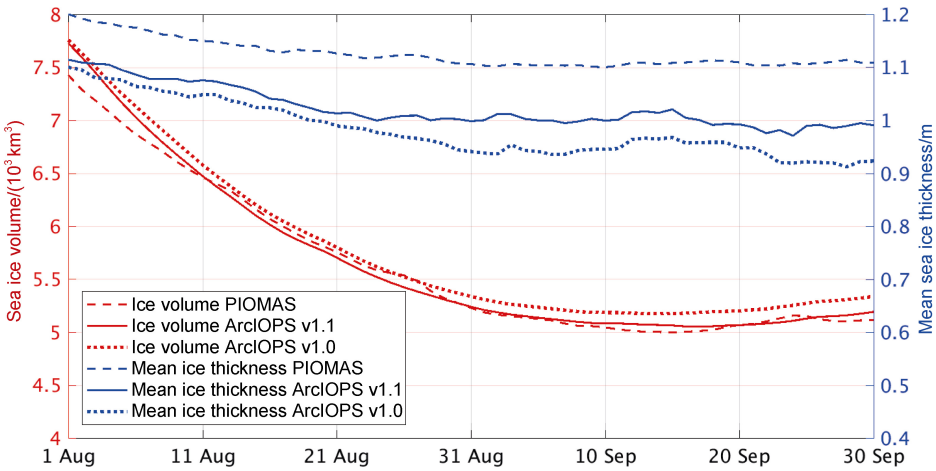

Figure 8 Time evolutions of the analyzed sea ice volume and mean thickness over the whole model domain. The blue and red lines denote the sea ice thickness and volume. The solid, dotted, and dashed lines denote the ArcIOPS v1.1, the v1.0 and the PIOMAS products, respectively. Mean thickness is calculated over the area where ice is thicker than 0.15 m.

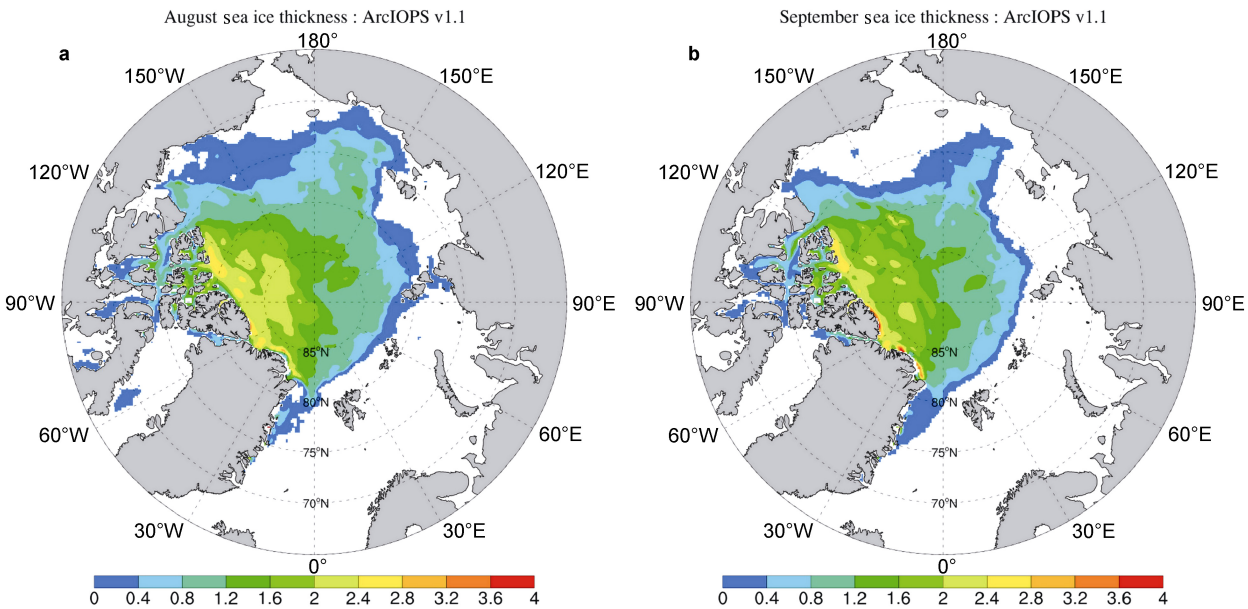

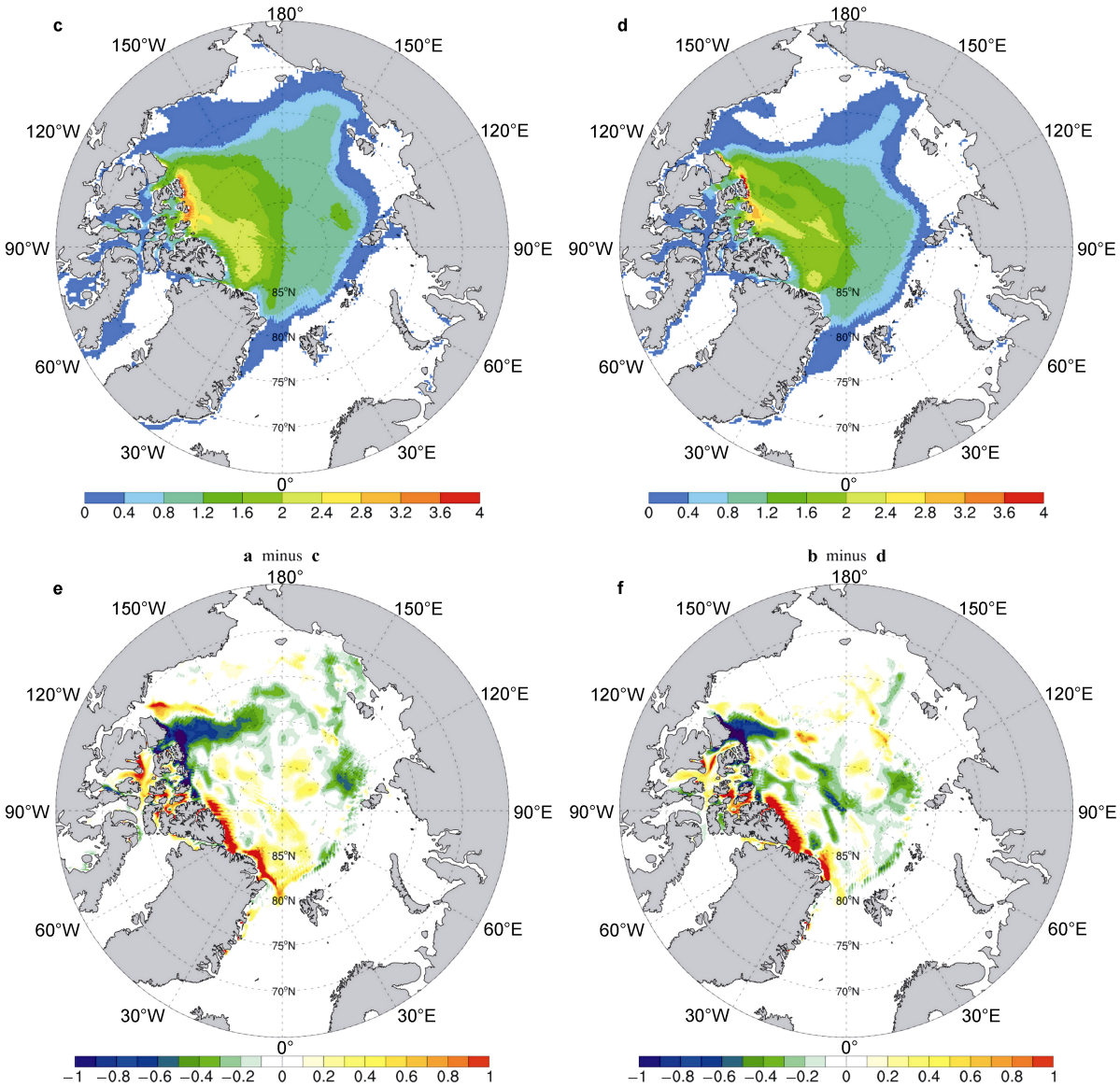

Figure 9 The mean analyzed sea ice thickness in August (**a**, **c**, **e**) and September (**b**, **d**, **f**). The top, middle, and bottom panels denote the ArcIOPS v1.1, the PIOMAS, and the deviation between the ArcIOPS v1.1 and PIOMAS products, respectively.

Currently, ArcIOPS v2.0 is under development in the NMEFC. The horizontal resolution of ArcIOPS v2.0 is 4.5 km. Satellite sea ice concentration, thickness and SST data are assimilated into ArcIOPS v2.0. In the future, more and more observations, such as T/S profiles, sea surface salinity and sea ice drift, will be assimilated into ArcIOPS, and sea ice and ocean forecasting products from ArcIOPS will continue to benefit Chinese scientific and commercial activities in the Arctic Ocean.

Acknowledgments This paper is a contribution to the Year of Polar Prediction (YOPP), a flagship activity of the Polar Prediction Project (PPP), initiated by the World Weather Research Programme (WWRP) of the World Meteorological Organization (WMO). The authors thank the University of Bremen for the AMSR2 data, the University of Hamburg for the SMOS data, the Alfred-Wegener-Institut, Helmholtz Zentrum für Polar- und Meeresforschung for the CryoSat-2 data, the Copernicus Marine Environment Monitoring Service for the GMPE SST data, the Norwegian Meteorological Institute for the OSISAF data, the Polar Research Institute of China for the EM31 data, and the University of Washington for the PIOMAS data. The authors thank the two anonymous reviewers for the constructive comments. This work is supported by the National Key R&D Program of China (Grant nos. 2016YFC1402700, 2017YFE0111700) and the National Natural Science Foundation of China (Grant no. 41506224).

References

Comiso J C, Cavalieri D J, Parkinson C L, et al. 1997. Passive microwave algorithms for sea ice concentration: a comparison of two techniques. Remote Sens Environ, 60(3): 357-384.

Crane R G. 1983. Atmosphere-sea ice interactions in the Beaufort/Chukchi

Sea and in the European sector of the Arctic. J Geophys Res Oceans, 88(C7): 4505-4523, doi: 10.1029/JC088iC07p04505.

Day J J, Hawkins E, Tietsche S. 2014. Will Arctic sea ice thickness initialization improve seasonal forecast skill? Geophys Res Lett, 41: 7566-7575.

Eastwood S, Larsen K R, Lavergne T, et al. 2011. Global sea ice concentration reprocessing. Product User Manual, EUMETSAT OSISAF, Document version 2.

Evensen G. 1994. Sequential data assimilation with a nonlinear quasi-geostrophic model using Monte Carlo methods to forecast error statistics. J Geophys Res, 99: 10143-10162.

Guo J, Sun B, Tian G, et al. 2008. Research on electromagnetic inductive measurement of sea-ice thickness in Antarctic Prydz Bay. Chinese J Geophys, 51(2): 596-602 (in Chinese with English abstract).

Kaleschke L, Maaβ N, Haas C, et al. 2010. A sea-ice thickness retrieval model for 1.4 GHz radiometry and application to airborne measurements over low salinity sea-ice. Cryosphere, 4: 583-592.

Kaleschke L, Tian-Kunze X, Maaβ N, et al. 2012. Sea ice thickness retrieval from SMOS brightness temperatures during the Arctic freeze-up period. Geophys Res Lett, 39: L05501.

Kwok R, Cunningham G F, Wensnahan M, et al. 2009. Thinning and volume loss of the Arctic Ocean sea ice cover: 2003-2008. J Geophys Res, 114(7), doi: 10.1029/2009JC005312.

Laxon S W, Giles K A, Ridout A L, et al. 2013. Cryosat-2 estimates of Arctic sea ice thickness and volume. J Geophys Res, 40(4): 732-737.

Liang X, Losch M. 2018. On the effects of increased vertical mixing on the Arctic Ocean and sea ice. J Geophys Res-Oceans, 123: 9266-9282.

Liang X, Losch M, Nerger L, et al. 2019. Using sea surface temperature observations to constrain upper ocean properties in an Arctic sea ice-ocean data assimilation system. J Geophys Res-Oceans, 124: 4727-4743.

Liang X, Yang Q, Nerger L, et al. 2017. Assimilating Copernicus SST Data into a Pan-Arctic Ice-Ocean Coupled Model with a Local SEIK Filter. J Atmos Ocean Tech, 34(9): 1985-1999.

Lisæter K A, Rosanova J, Evensen G. 2003. Assimilation of ice concentration in a coupled ice-ocean model using the ensemble Kalman filter. Ocean Dyn, 53: 368-388.

Losch M, Menemenlis D, Campin J M, et al. 2010. On the formulation of sea-ice models. Part 1: Effects of different solver implementations and parameterizations. Ocean Model, 33: 129-144.

Marshall J, Adcroft A, Hill C, et al. 1997. A finite-volume, incompressible Navier Stokes model for studies of the ocean on parallel computers. J Geophys Res, 102(C3): 5753-5766.

Mu L, Yang Q, Losch M, et al. 2018a. Improving sea ice thickness estimates by assimilating cryosat-2 and smos sea ice thickness data simultaneously. Q J R Meteorol Soc, 144(711): 529-538.

Mu L, Losch M, Yang Q, et al. 2018b. Arctic-wide sea-ice thickness estimates from combining satellite remote sensing data and a dynamic ice-ocean model with data assimilation during the CryoSat-2. J Geophys Res-Oceans, 123: 7763-7780.

Mu L, Liang X, Yang Q, et al. 2019. Arctic ice ocean prediction system: evaluating sea ice forecasts during *Xuelong*'s first trans-Arctic passage in summer 2017. J Glaciol, doi: 10.1017/jog.2019.55.

Nerger L, Hiller W. 2013. Software for ensemble-based data assimilation systems-implementation strategies and scalability. Comput Geosci, 55: 110-118.

Nerger L, Janji T, Schröter J, et al. 2012. A unification of ensemble square root Kalman filters. Mon Weather Rev, 140(7): 2335-2345.

Nguyen A T, Menemenlis D, Kwok R. 2011. Arctic ice-ocean simulation with optimized model parameters: Approach and assessment. J Geophys Res, 116: C04025.

Ricker R, Hendricks S, Helm V, et al. 2014. Sensitivity of CryoSat-2 Arctic sea ice freeboard and thickness on radar-waveform interpretation. Cryosphere, 8(4): 1607-1622.

Ricker R, Hendricks S, Kaleschke L, et al. 2017. A weekly Arctic sea-ice thickness data record from merged CryoSat-2 and SMOS satellite data. Cryosphere, 11: 1607-1623.

Sakov P, Counillon F, Bertino L, et al. 2012. TOPAZ4: An ocean-sea ice data assimilation system for the North Atlantic and Arctic. Ocean Sci, 8: 633-656.

Semtner A J J. 1976. A model for the thermodynamic growth of sea ice in numerical investigations of climate. J Phys Oceanogr, 6(3): 379-389.

Smith W H F, Sandwell D T. 1997. Global sea floor topography from satellite altimetry and ship depth soundings. Science, 277(5334): 1956-1962.

Spreen G, Kaleschke L, Heygster G. 2008. Sea ice remote sensing using AMSR-E 89 GHz channels. J Geophys Res, 113: C02S03.

Thorndike A S, Colony R. 1982. Sea ice motion in response to geostrophic winds. J Geophys Res-Oceans, 87: C8.

Tian-Kunze X, Kaleschke L, Maaβ N, et al. 2014. SMOS-derived thin sea ice thickness: Algorithm baseline, product specifications and initial verification. Cryosphere, 8: 997-1018.

Wingham D J, Francis C R, Baker S, et al. 2006. Cryosat: A mission to determine the fluctuations in Earth's land and marine ice fields. Adv Sp Res, 37(4): 841-871.

Yang J, Comiso J, Walsh D, et al. 2004. Storm-driven mixing and potential impact on the Arctic Ocean. J Geophys Res, 109: C04008.

Yang Q, Losa S N, Losch M, et al. 2014. Assimilating SMOS sea ice thickness into a coupled ice-ocean model using a local SEIK filter. J Geophys Res-Oceans, 119: 6680-6692.

Yang Q, Losa S N, Losch M, et al. 2015. Assimilating summer sea-ice concentration into a coupled ice-ocean model using a LSEIK filter. Ann Glaciol, 56(69): 38-44.

Zhang J, Rothrock D A. 2003. Modeling global sea ice with a thickness and enthalpy distribution model in generalized curvilinear coordinates. Mon Weather Rev, 131(5): 845-861.